The Effects of Resistive Loading of "TEM" Horns

MOTOHISA KANDA, MEMBER, IEEE

Abstract—**A short transverse electromagnetic (TEM) horn with continuously tapered resistive loading was developed for directional reception or transmission of picosecond pulses with minimal distortion. It was found to be broadband and nondispersive with a low VSWR. The receiving transient response of the resistively loaded "TEM" horn indicates that the waveform of a 70-ps impluse is well preserved. The theoretical analyses using the method of moments and the fast Fourier transform (FFT) technique were performed and agreed well with time-domain measurements.**

Key Words—**Broadband; directivity; effective length; FFT; method of moments; nondispersive; picosecond pulse; resistive loading; TEM horn; transfer function; transient.**

I. INTRODUCTION

RECENT study related to electromagnetic-pulse (EMP) phenomena has focused strong attention on the subject of transient electromagnetic (EM) fields. Antenna structures able to preserve the time-domain waveform of EMP must be inherently broadband and nondispersive. One such antenna, which has been successfuly fabricated, is a dipole with continuously tapered resistive loading [1], [2].

In an effort to attain increased directivity or increased antenna gain for a broadband and nondispersive antenna, many researchers have considered a transverse electromagnetic (TEM) horn, which is a two-conductor, end-fire traveling-wave structure. If the flare angle and the plate widths of a TEM horn are properly chosen so that a constant, characteristic impedance can be maintained, the horn will guide an essentially TEM mode into free space. Thus a TEM horn can be considered as a transition section which transfers EM energy from a transmission line to free space. In order to achieve a "smooth" transition, i.e., a transition with low reflection, the length of a conventional conductive TEM horn has to be at least one-half wavelength long at the lowest frequency of interest. This means that if the lowest frequency of interest is 100 MHz, a TEM horn may be as long as 1.5 m, which is too long to be practical.

The Cornell Aeronautical Laboratory (CAL) designed a TEM horn with nonuniform-line matching from 50 Ω at the antenna throat to 377 Ω at the aperture. The nonuniform-line matching was achieved by forming the TEM horn plates into empirically determined tear-drop shapes. A small resistance-card termination was placed at the tip of the aperture to provide adequate current attenuation for a traveling wave. With these empirical modifications, the length of the TEM horn was reduced to 1 m with a reasonable reflection coefficient (less than 0.48) for the frequency range of 100 MHz to 2 GHz.

In this paper, a "TEM" horn with continuously tapered resistive loading is considered for the purpose of developing a relatively short, broadband and nondispersive antenna with high directivity. One-dimensional, theoretical analysis for a resistively loaded "TEM" horn using the method of moments [3] has been performed in the frequency domain. The fast Fourier transform (FFT) technique then allows the determination of transient radiated EM fields for a known input-pulse waveform. Comparison between theory and time-domain measurements is also given in this paper.

Manuscript received September 2, 1981; revised January 11, 1982.

The author is with the Electromagnetic Fields Division, National Bureau of Standards, Boulder, CO 80303. (303) 497-5320.

II. THEORETICAL CONSIDERATIONS

In this section, the theoretical considerations for a one-dimensional model of a resistively loaded "TEM" horn, as shown in Fig. 1, are given first. A one-dimensional analysis simplifies the mathematics involved, yet gives good physical insight for evaluating the effects of resistive loading on a TEM horn.

Then, a conductive TEM horn is analyzed using the biconical antenna model given in Fig. 2. By adjusting the apex angle and the lengths of the cones, this model gives good physical understanding for analyzing conductive TEM horns.

A. A Resistively Loaded "TEM" Horn

Because of the presence of loss in TEM-horn plates, the field patterns for EM waves propagating between lossy plates deviate from a pure TEM mode. Since a resistively loaded "TEM" horn cannot support a pure TEM mode, the term "TEM" horn may not be truly appropriate but will be used throughout this paper.

If there are abrupt changes in the characteristics of the boundary (i.e., air to lossy-TEM-horn plate), the problem can be solved by finding general solutions for each of the regions and evaluating unknown constants by satisfying the boundary conditions across plate interfaces. A transcendental matrix equation derived by matching the field across the plate interface is likely to be difficult to solve in general cases. Therefore, this paper analyzes a one-dimensional model given in Fig. 1, which ignores any transverse current components on the lossy plates. When the horn angle is constant and the plates taper smoothly, it is a reasonable assumption to neglect transverse components of current on the lossy plates. The shape for horn plates in the study is, therefore, chosen to be triangular.

Using the one-dimensional model which neglects any transverse component of current on the lossy plate, we calculate numerically the longitudinal component of the

0018-9375/82/0500-0245$00.75 © 1982 IEEE

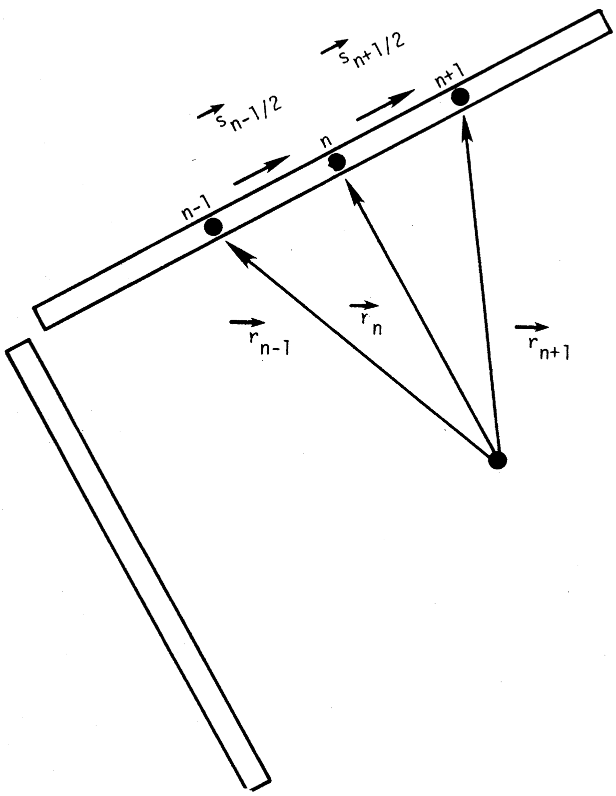

Fig. 1. One-dimensional model for a resistively loaded "TEM" horn.

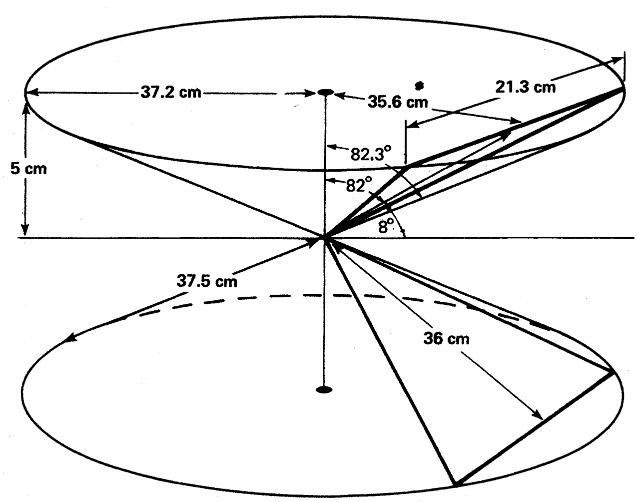

Fig. 2. Biconical model for a conductive TEM horn. (Dimensions in centimeters.)

current by using the method of moments. In this paper, we review briefly a general theoretical development for a one-dimensional, resistively loaded antenna structure, which can be bent and can have step discontinuities in radius. More detailed discussion on the theory is given elsewhere [3], [4].

Fig. 1 shows a typical one-dimensional structure of a TEM horn modeled by a V antenna with a resistive section. Using a one-dimensional model, the current is assumed to be uniform perpendicular to the figure and to flow in one direction on each plate. Then, the incident electrical field E_{inc} associated with the current I and the charge density ρ on a one-dimensional plate are given in terms of the usual vector and scalar potentials $\vec{A}$ and Φ

$$\vec{E}_{\text{inc}} = -j\omega A - \nabla\Phi, \tag{1}$$

$$\vec{A} = \frac{\mu}{4\pi} \int_c I(s')\vec{s}(s') \frac{e^{-jkR}}{R}\, ds' \tag{2}$$

and

$$\Phi = \frac{1}{4\pi\epsilon} \int_c \rho(s') \frac{e^{-jkR}}{R}\, ds' \tag{3}$$

where R is defined to be

$$R = \sqrt{|\vec{r} - \vec{r}'(s')|^2 + a^2(s')}. \tag{4}$$

One-dimensional charge density $\rho(s)$ is related to the current $I(s)$ through the equation of continuity

$$\rho(s) = \frac{-1}{j\omega}\frac{dI(s)}{ds}. \tag{5}$$

The unit direction vector $\vec{s}$, which is parallel to the axis of each segment, is defined as

$$\vec{s}_{n+1/2} = \frac{\vec{r}_{n+1} - \vec{r}_n}{|\vec{r}_{n+1} - \vec{r}_n|}. \tag{6}$$

Using the pulse-testing function, expanding the current in pulses, and applying a finite-difference approximation to compute charge density ρ, we can rearrange (1) in terms of the usual impedance matrix Z_{mn} associated with the current and voltage matrix I_n and V_m, i.e.,

$$\sum_{n=1}^{N} I_n Z_{mn} = V_m. \tag{7}$$

The matrix element Z_{mn} associated with the nth current at the observation s_m is given by [4]

$$\begin{aligned} Z_{mn} = \frac{-1}{4\pi j\omega\epsilon} & k^2(\vec{r}_{m+1/2} - \vec{r}_{m-1/2}) \\ & \cdot (\vec{s}_{n+1/2}\Psi_{m,n,n+1/2} + \vec{s}_{n-1/2}\Psi_{m,n-1/2,n}) \\ & - \frac{\Psi_{m+1/2,n,n+1}}{s_{n+1} - s_n} + \frac{\Psi_{m+1/2,n-1,n}}{s_n - s_{n-1}} \\ & + \frac{\Psi_{m-1/2,n,n+1}}{s_{n+1} - s_n} - \frac{\Psi_{m-1/2,n-1,n}}{s_n - s_{n-1}} \\ & + Z(s_m)(s_{m+1/2} - s_{m-1/2}) \end{aligned} \tag{8}$$

where $Z(s_m)$ is the internal resistance per unit length due to resistive loading. Both the vector and scalar potential terms involve the integral of the form

$$\Psi_{m,\mu,v} = \int_{s_\mu}^{s_v} \frac{e^{-jkR_m}}{R_m}\, ds' \tag{9}$$

where

$$R_m = \sqrt{|\vec{r}_m - \vec{r}'(s')|^2 + a^2(s')}. \tag{10}$$

The matrix element V_m is simply given by

$$V_m = \vec{E}^{\mathrm{inc}}(s_m) \cdot (\vec{r}_{m+1/2} - \vec{r}_{m-1/2}). \tag{11}$$

The resistive-loading profile $Z(s)$ in ohms per meter of a "TEM" horn is expressed as

$$Z(s) = \frac{Z_0}{1 - \dfrac{s}{l}} \quad \Omega/\mathrm{m}, \qquad 0 \leqslant s \leqslant l \tag{12}$$

where Z_0 is the resistance per unit length (Ω/m) at the driving point, and l is the length of the "TEM" horn. Equation (12) predicts that the resistive loading of the "TEM" horn increases continuously from the value $Z_0(\Omega/\mathrm{m})$ at the driving point to infinity at the end of the "TEM" horn. This particular resistive-loading profile, which enables a TEM horn to handle extremely-wide-bandwidth signals without dispersion distortion, has been chosen by many researchers [5]-[8] as well as by the author [1], [2]. In essence, there exists a critical value for Z_0, for which a "TEM" horn can sustain a traveling-wave current from the driving point toward the end of the "TEM" horn. A traveling-wave structure supporting TEM-mode propagation is essential for transmitting and receiving a signal with large instantaneous bandwidth without serious pulse broadening or wide-angle sidelobes.

Once the current distribution of the resistively loaded "TEM" horn is determined, the effective length $h_e(f)$ of the antenna can be calculated from the moment of its current distribution divided by the driving-point current, i.e.,

$$h_e(f) = \frac{1}{I_z(0)} \int_0^l I_z(z')\, dz'. \tag{13}$$

The effective length and the driving-point impedance of the antenna are required later to evaluate its transfer function.

A formal solution to the resistively loaded "TEM" horn problem can be formulated by modeling solid-plate surfaces with loaded wire grids or meshes. This extends the one-dimensional problem to a two- or three-dimensional problem by taking into account the transverse current components on horn plates. The moment-method technique will give a reasonable solution in the frequency range in which each surface is smaller than a few square wavelengths. Above those frequencies, the moment method unfortunately needs many loaded wire segments, and, therefore, requires many unknown currents to model a solid surface accurately. In this case, perhaps the geometrical-theory-of-diffraction (GTD) technique would provide more efficient solutions to this problem. These techniques will be pursued for better understanding of a resistively loaded "TEM" horn.

In the present study, the one-dimensional theoretical analysis for the resistively loaded "TEM" horn using the method of moments [3] has been performed in the frequency domain. Using the FFT then allows the determination of transient characteristics of the antenna.

B. Conductive TEM Horns

In a previous paper [9], [10], the author developed a simple theoretical model using the assumed aperture field. In this model, the horn flare angle and the plate widths are chosen so that the TEM horn guides only the TEM mode by maintaining a constant impedance. If the edge diffraction effect and fringe fields are neglected, the aperture field of the TEM horn is assumed to be a linearly polarized, spherical field. Once an aperture field is established, the radiated EM field at any distance can be evaluated using the plane-wave spectrum analysis technique.

As discussed in [9], [10], a number of major limitations of the simplified theoretical model still remain, although some useful engineering design concepts were obtained. For example, the assumption that a TEM mode is basically guided from the throat to the aperture by the nondispersive TEM horn is highly questionable. Particularly at the high frequency range of the spectrum, above 1 GHz for example, the aperture field may be quite different from a basic TEM mode due to higher modes. Even at the lower frequency ranges, below 1 GHz for example, the magnitude of the TEM mode at the aperture may not remain constant due to a high reflection coefficient, e.g., 0.98 at 100 MHz.

In an effort to treat these aspects more rigorously, a formal solution to the TEM-horn problem using a vector integral-equation technique was proposed. Using the equivalence principle [11], the electric field $\vec{E}$ in free space generated by an unknown set of electric currents $\vec{J}$ on the TEM-horn plates is

$$\vec{E} = -\nabla \times \vec{F} - j\omega\mu\vec{A} + \frac{1}{j\omega\epsilon}\nabla(\nabla \cdot \vec{A}) \tag{14}$$

where the electric vector potential $\vec{F}$ is given in terms of the known excitation equivalent magnetic current $\vec{M}$ by

$$\vec{F} = \frac{1}{4\pi} \int_{\mathrm{source}} \vec{M}\, \frac{e^{-jkR}}{R}\, ds \tag{15}$$

and the magnetic vector potential $\vec{A}$ is given in terms of the unknown current $\vec{J}$ on the TEM-horn plates by

$$\vec{A} = \frac{1}{4\pi} \int_{\mathrm{plates}} \vec{J}\, \frac{e^{-jkR}}{R}\, ds \tag{16}$$

with $R = |r - r'|$.

Boundary conditions are such that the tangential electric field at the TEM horn plates is zero, i.e.,

$$\vec{n} \times \vec{E} = 0 \,|_{\text{on the plates.}} \tag{17}$$

Substituting (14), (15), and (16) into (17) gives

$$\begin{aligned} &\vec{n} \times \left(-\nabla \times \frac{1}{4\pi} \iint \vec{M} \frac{e^{-jkR}}{R}\, ds \right) \\ &+ \vec{n} \times \left[-\frac{j\omega\mu}{4} \iint \vec{J} \frac{e^{-jkR}}{R}\, ds \right. \\ &\left. + \frac{1}{j\omega\epsilon} \nabla \left(\nabla \times \frac{1}{4\pi} \iint \vec{J} \frac{e^{-jkR}}{R}\, ds \right) \right] \\ &= 0 \,|_{\text{on the plates.}} \end{aligned} \tag{18}$$

The above electric-field integral equation may be solved for the unknown $\vec{J}$. Once $\vec{J}$ is determined, the other EM fields everywhere may be determined by use of (14)–(16).

The derivation of the electric-field integral equation given in (18) is complete and straightforward. The solution may be obtained using the method-of-moments technique. The horn plates are divided into small patches. After the vector integral equation given in (18) is decomposed into appropriate, coupled, scalar integral equations, two orthogonal components of current $\vec{J}$ with two unknown constants over each patch must be forced to satisfy the boundary condition. Although the matrix formulations of the problem are quite straightforward, their solution can be extremely formidable, particularly at higher frequencies where each patch has to be subdivided into patches small compared to a wavelength. Although some symmetry arguments may be used to keep the matrix sizes tractable, there is no easy way out except to perform a very large matrix computation. In addition, because the FFT is used to obtain the transient characteristics of the TEM horn, the above electric-field integral equation has to be solved for many frequency points, e.g., on the order of one thousand from 10 MHz to several gigahertz. This is a very expensive process.

In this paper, a simple model, modified from one used in previous papers by the author [9], [10], is adopted to analyze a conductive TEM horn. The model used here is a biconical antenna structure, where the apex angle and the length of a bicone are adjusted to fit a TEM horn. The biconical model of a conducting TEM horn is shown in Fig. 2. A knowledge of both the driving-point impedance and the effective length of the antenna for the frequency range over which the spectrum of the excitation has significant amplitude is required to discuss quantitatively the transient response of a transmitting and receiving TEM horn using the FFT technique.

The effective length $h_e(f)$ and the driving-point impedance $Z_0(f)$ of a wide-angle conical antenna, studied by many workers [12] as well as by the author [9], [10], are given respectively by

$$\begin{aligned} h_e(f) = &\frac{1}{k^2 l \left(1 + \frac{\beta}{\alpha}\right)} \left(\frac{\beta}{\alpha} e^{jkl} - e^{-jkl} \right) \\ &\cdot \sum_{n=1,3,5}^{\infty} P_n(\cos\theta_0) P_n^{\,1}(0) \left(\frac{2n+1}{n^2+n} \right) \\ &\cdot \frac{j^{n+1}}{h_{n-1}^{(2)}(kl) - \frac{n}{ka} h_n^{(2)}(kl)} \end{aligned} \tag{19}$$

and

$$Z_0(f) = Z_c \left(\frac{1 - \frac{\beta}{\alpha}}{1 + \frac{\beta}{\alpha}} \right). \tag{20}$$

The symbols have the following meanings:

l is the length of the antenna,

$P_n(\cos\theta)$ is the Legendre polynomial of order n,

$h_n^{(2)}(kl)$ is the spherical Hankel function of the second kind

$$Z_c = 120 \ln \cot \frac{\theta_0}{2} \tag{21}$$

$$\begin{aligned} \frac{\beta}{\alpha} &= e^{-j2kl} \\ &\cdot \left\{ \frac{1 + j\dfrac{120}{Z_c} \displaystyle\sum_{n=1}^{\infty} \frac{2n+1}{n(n+1)} [P_n(\cos\theta_0)]^2 \zeta_n(kl)}{-1 + j\dfrac{120}{Z_c} \displaystyle\sum_{n=1}^{\infty} \frac{2n+1}{n(n+1)} [P_n(\cos\theta_0)]^2 \zeta_n(kl)} \right\} \end{aligned} \tag{22}$$

and

$$\zeta_n(kl) = \frac{h_n^{(2)}(kl)}{h_{n-1}^{(2)}(kl) - \frac{n}{kl} h_n^{(2)}(kl)}. \tag{23}$$

Then the far-field electric field is given by

$$E(f) = j \frac{60\, V_g}{Z_0(f) + Z_g} F(f) \frac{e^{-jkr}}{r} \tag{24}$$

where the field characteristic $F(f)$ is related to the effective length $h_e(f)$ through the Rayleigh–Carson reciprocity theorem [13]

$$F(f) = k h_e(f). \tag{25}$$

III. CHARACTERISTICS OF RESISTIVELY LOADED "TEM" HORNS

A. Loading Profile

In the present study, the one-dimensional theoretical analysis for a triangularly shaped "TEM" horn with resistive

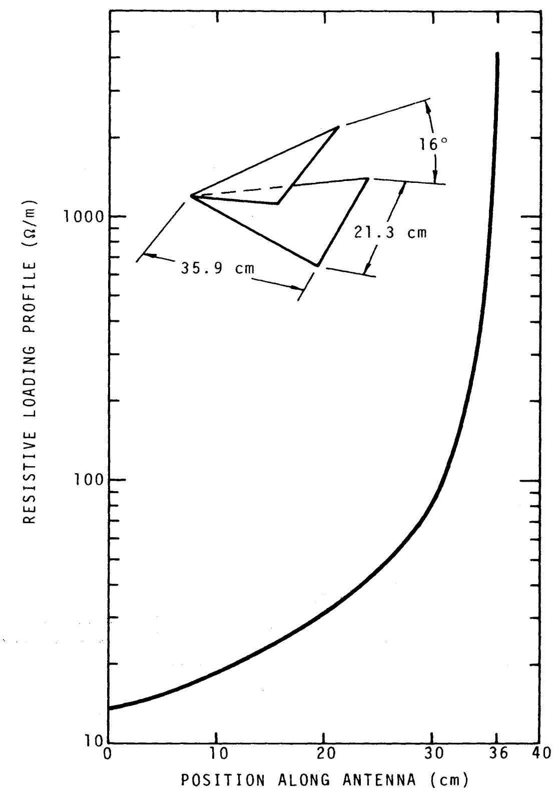

Fig. 3. Resistively loaded "TEM" horn.

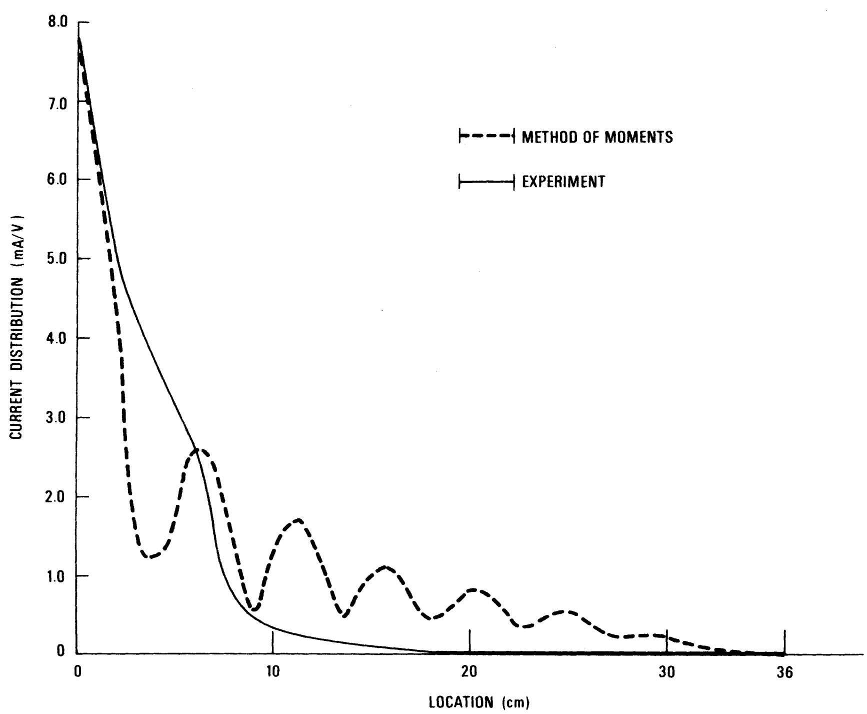

Fig. 4. Current distribution of a resistively loaded "TEM" horn.

loading has been performed to solve for the current distribution using the method of moments. The physical dimensions of the TEM horn are shown in Fig. 3.

If Z_0 in (12) is chosen to be about 14 Ω/m, then a 36-cm long "TEM" horn can sustain a traveling-wave current along the antenna for the frequency range of 100 MHz to 8 GHz. When Z_0 is lower than 14 Ω/m, the current distributions along the antenna are similar to standing waves. On the other hand,

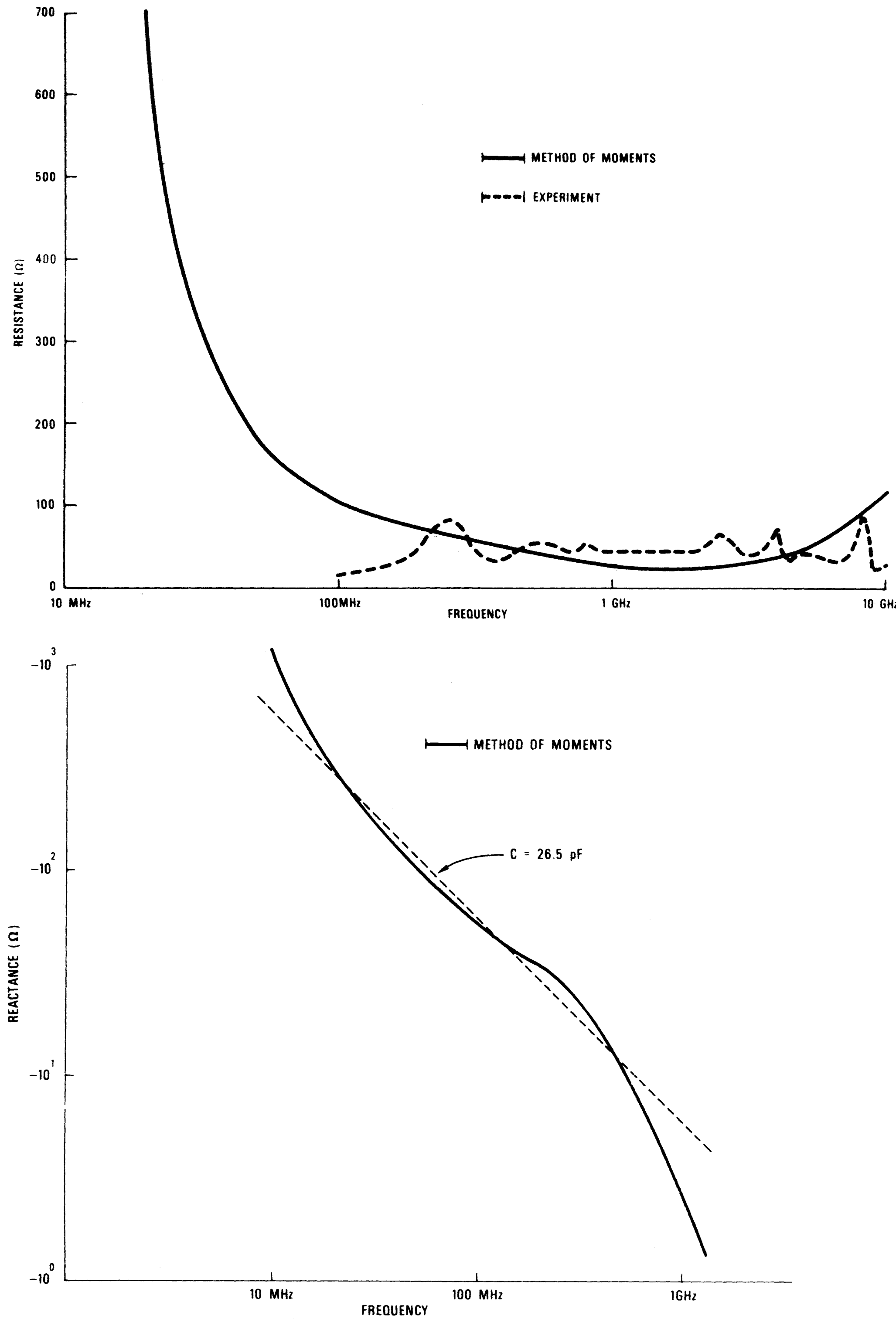

Fig. 5. Driving point impedance of a resistively loaded "TEM" horn.

when Z_0 is much higher than 14 Ω/m, the current distribution is overdamped, and the radiation efficiency of the antenna is expected to be very low because the antenna is acting like a load termination.

Several resistively loaded "TEM" horns have been made by sputtering copper on polycarbonate substrates ($\epsilon_r \cong 3$). The required resistive-loading profile was obtained by moving the substrate through a stationary mask.

B. Current Distribution

The current distributions on the resistively loaded, 36-cm long "TEM" horn are calculated numerically using the method of moments for the frequency range of 10 MHz to 5 GHz. The discussion of the numerical technique used to calculate the current distribution on the resistively loaded "TEM" horn was given briefly in Section II-A.

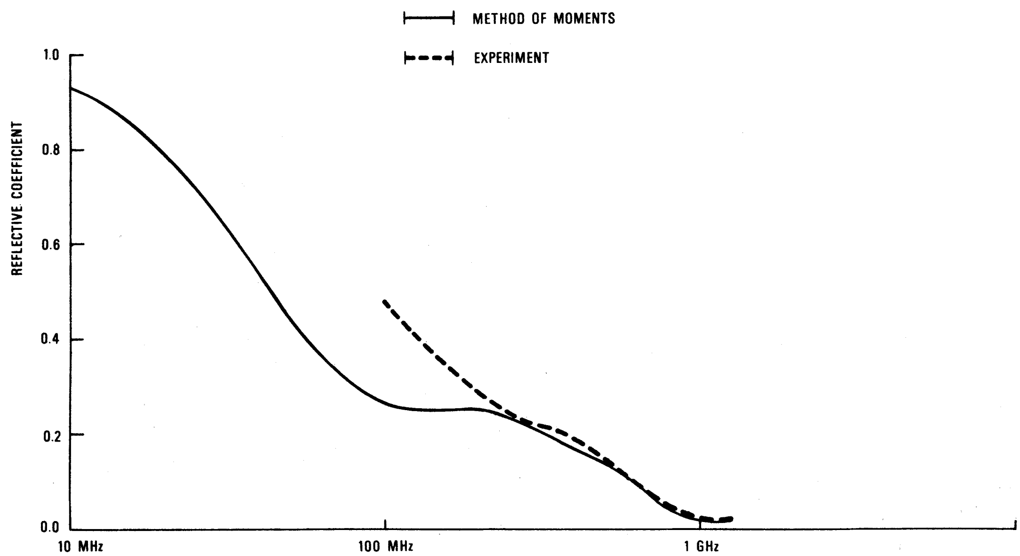

Fig. 6. Reflection coefficient of a resistively loaded "TEM" horn.

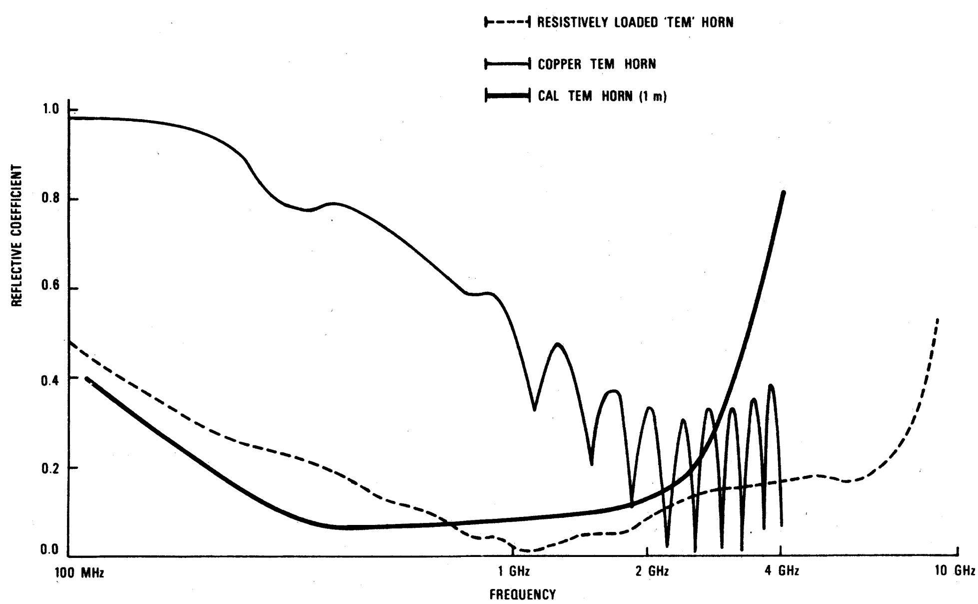

Fig. 7. Measured reflection coefficients of various "TEM" horns.

The current distribution at frequencies above 100 MHz is a traveling wave, whereas that below 100 MHz exhibits a standing-wave component due to a reflection from the end. Fig. 4 shows the current distribution at 1 GHz along with the experimental results. The current distribution measurement was made using a 1-cm-diameter loop with a beam-lead Schottky diode. The discrepancy between theoretical and experimental results is mainly due to experimental difficulties encountered in measuring current distribution using the electrically small loop antenna.

C. Driving-Point Impedance

Fig. 5 shows the driving-point resistance and reactance obtained by the method of moments along with the experimental results. The experimental results were obtained using an automatic network analyzer. The impedance of the resistively loaded "TEM" horn typically has a resistance of about 70 Ω and a capacitance of about 27 pF in a series configuration.

D. Reflection Coefficient

The input reflection coefficient of the 36-cm-long resistively loaded "TEM" horn is shown in Fig. 6. The reflection coefficient typically stays below 0.5 for the frequency range from 100 MHz to 8 GHz as shown in this figure. For comparison, the reflection coefficients of a 36-cm-long conducting TEM horn and a 1-m-long CAL TEM horn are also shown in Fig. 7. This figure indicates that the reflection coefficient of the TEM horn has been significantly improved through resistive loading, and that the reflection coefficient of the 36-cm-long resistively loaded "TEM" horn is comparable to that of a 1-m-long CAL TEM horn. On the other hand, the reflection coefficient of a conducting TEM horn is very high, particularly at the low-frequency range (0.98 at

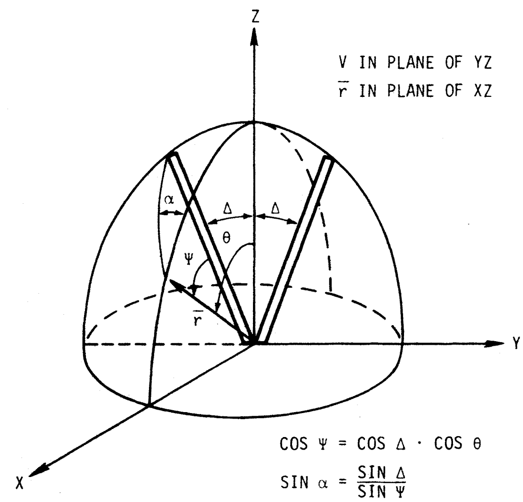

Fig. 8. Geometry for a resistively loaded "TEM" horn.

100 MHz), and shows an oscillatory nature above 1 GHz due to interference between reflection from the aperture and reflection from the feed point.

E. Radiation Power Pattern

To obtain the far-field radiation power pattern of the resistively loaded "TEM" horn, it is assumed that the current flows in the branches of the antenna, and that transverse components of current are ignored. Once the current distribution of the antenna is determined, the far-field radiation power pattern $E_{\|}{}^{r}$ in the E plane is given by

$$E_{\|}{}^{r}(\theta) = j\omega \sin(\theta - \Delta/2) \frac{\mu_0 e^{-jkr}}{4\pi r} \cdot \int I_z(z') e^{-jkz' \cos(\theta - \Delta/2)}\, dz' - j\omega \sin(\theta + \Delta/2) \frac{\mu_0 e^{-jkr}}{4\pi r} \cdot \int I_z(z') e^{-jkz' \cos(\theta + \Delta/2)}\, dz'. \tag{26}$$

The far-field radiation power pattern $E_{\perp}{}^{r}$ in the H plane is given by

$$E_{\perp}{}^{r}(\theta) = 2 \sin\alpha\, E_{\|}{}^{r}(\theta) \tag{27}$$

where

$$\sin\alpha = \frac{\sin\Delta}{\sqrt{1 - \cos^2\theta \cdot \cos^2\Delta}}. \tag{28}$$

The geometry considered is shown in Fig. 8. The theoretical results of far-field power patterns in the E and H planes are shown respectively in Figs. 9 and 10.

Experiments to measure radiation power patterns of the antenna in both the E and H planes were performed in an anechoic room using a standard horn as a transmitting antenna. The results are also shown in Figs. 9 and 10. It is found from these figures that the half-power beamwidths of the antenna are typically 100° in both E and H planes at 1 GHz. The directivity of the antenna is then estimated to be about 6 dB at 1 GHz.

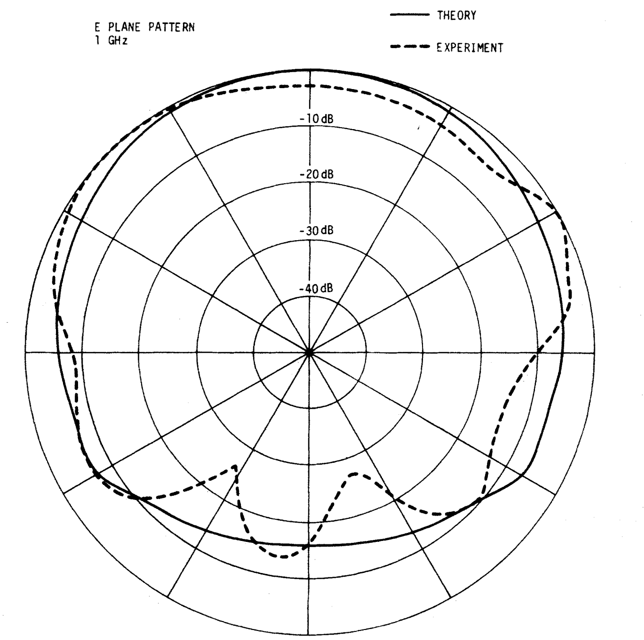

Fig. 9. Radiation power patterns in the E plane of a resistively loaded "TEM" horn.

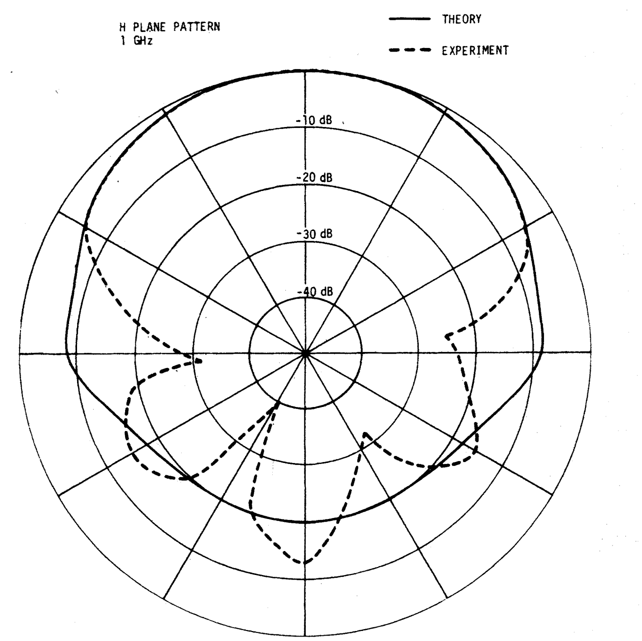

Fig. 10. Radiation power patterns in the H plane of a resistively loaded "TEM" horn.

IV. FREQUENCY-DOMAIN RESULTS

The frequency-domain representation of the receiving transfer function $S_r(f)$ of the resistively loaded "TEM"

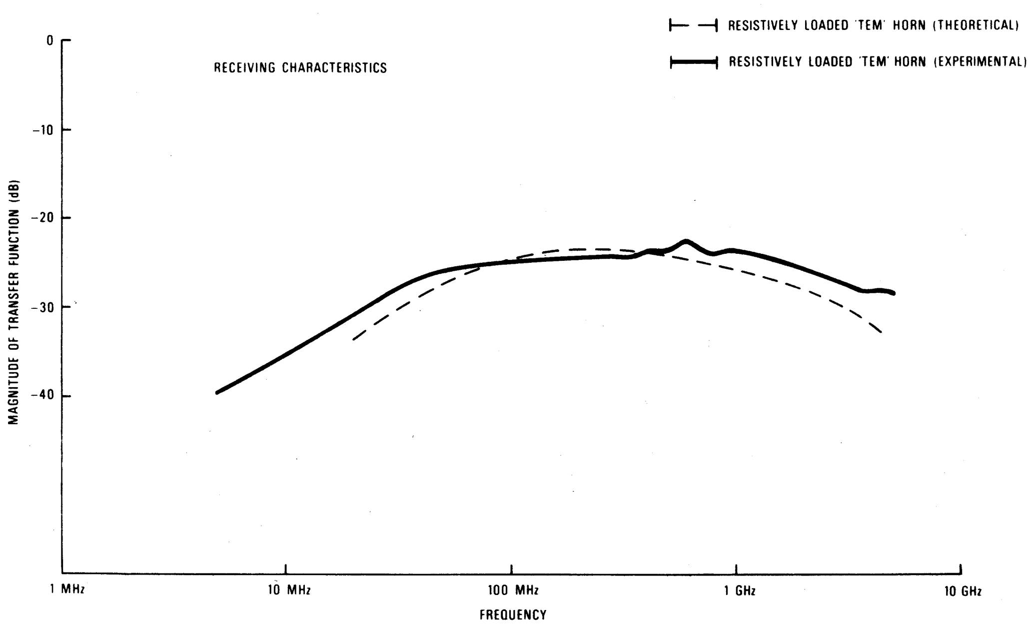

Fig. 11. Transfer function of a resistively loaded "TEM" horn.

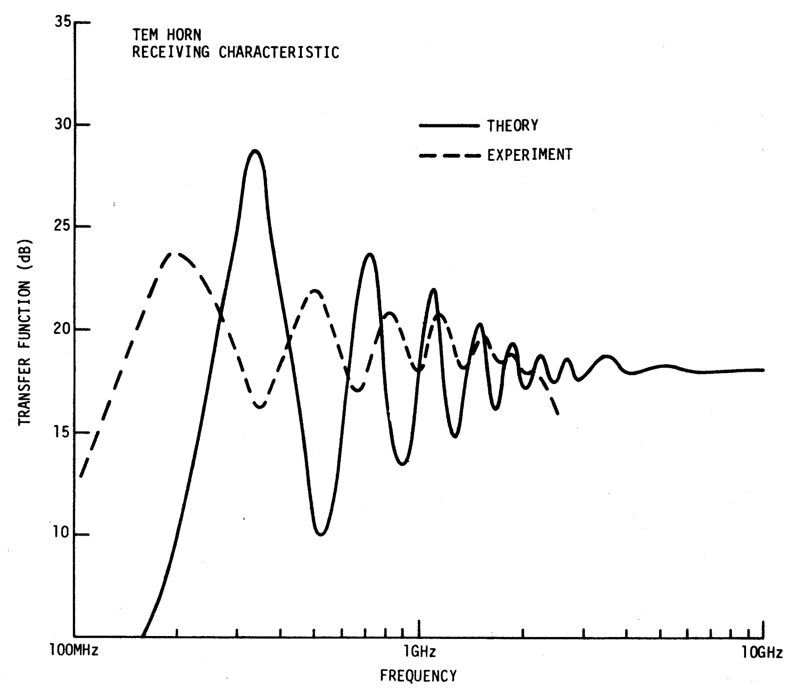

Fig. 12. Transfer function of a conductive TEM horn.

horn is given by

$$S_r(f) = \frac{V_L(f)}{E_{\text{inc}}(f)} = \frac{-h_e(f) Z_L(f)}{Z_0(f) + Z_L(f)} \tag{29}$$

where $V_L(f)$ is the load voltage (V), E_{inc} is the normal incident electric field (V/m), $h_e(f)$ is the effective length of the antenna (m), $Z_0(f)$ is the driving-point impedance of the antenna (Ω), and $Z_L(f)$ is the load impedance (Ω).

Using the effective length of the antenna (which is defined as the moment of its current distribution derived from the input current) and the driving-point impedance of the antenna, we calculate the frequency-domain representation of the receiving transfer function of the antenna using (29). The receiving transfer functions of the resistively loaded "TEM" horn and the conductive TEM horn are shown in Figs. 11 and 12, respectively.

Experiments were performed using a time-domain antenna range with a time-domain automatic network analyzer. The time-domain representation has been converted to the frequency-domain representation using the fast Fourier transform (FFT) technique. The measured receiving

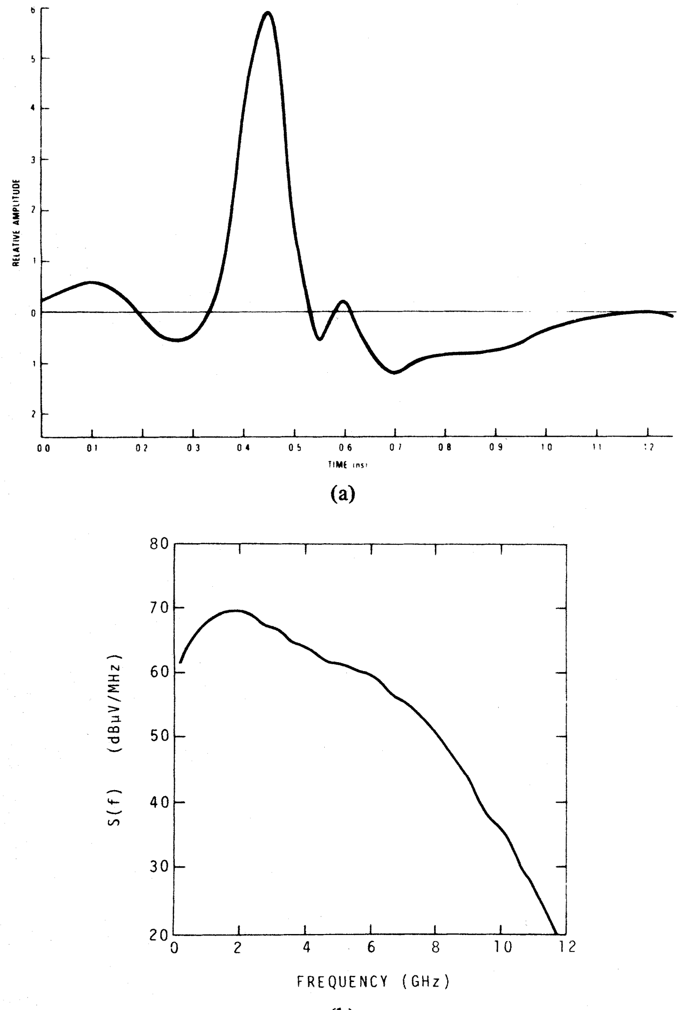

Fig. 13. Time-domain measurement. (a) Time-domain picosecond impulse. (b) Spectrum amplitude of picosecond pulse.

transfer function of the resistively loaded "TEM" horn and that of a conductive TEM horn of the same size are also shown in Figs. 11 and 12, respectively.

The theoretical and experimental results for the receiving transfer function of the resistively loaded "TEM" horn agree well. The receiving transfer function of the antenna is flat to within ±3 dB from 20 MHz to 7 GHz. On the other hand, the experimental results of the transfer function for a conducting TEM horn indicate that there are strong resonances in the horn and that its transfer function is not nearly as flat as that of the resistively loaded "TEM" horn.

V. TIME-DOMAIN RESULTS

Once frequency-domain solutions are determined, transient fields for a known input waveform can be found using the FFT technique. The experiments were performed using a time-domain antenna range with a time-domain automatic network analyzer. The impulse generator generates extremely short impulses (70 ps) with flat spectrum amplitudes greater than 60 dBV/MHz up to 5 GHz, as shown in Fig. 13. The 70-ps impulse was used both as a driving voltage for the investigation of transmitting transient responses and as an incident impulse

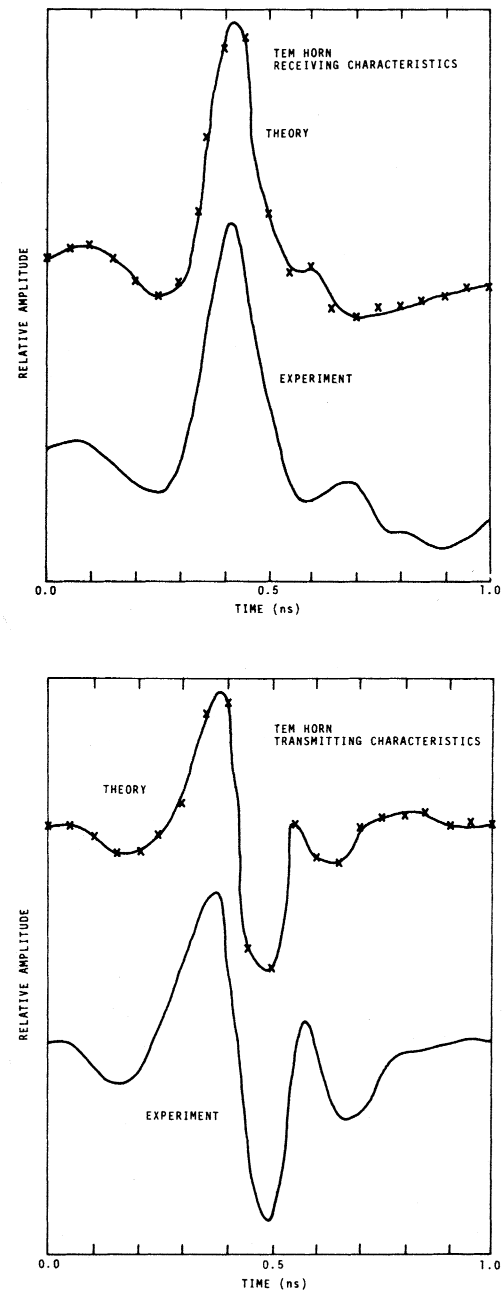

Fig. 14. Time-domain response of a resistively loaded "TEM" horn.

field for the investigation of receiving transient responses. Fig. 14 shows good agreement between the theoretical and experimental transient characteristics of receiving and transmitting responses for the resistively loaded "TEM" horn.

VI. CONCLUSION

For directional reception or transmission of picosecond pulses with minimal distortion, a short "TEM" horn with continuously tapered, resistive loading was developed, and was found to be broadband and nondispersive with a low VSWR. The receiving transient response of the resistively loaded "TEM" horn indicates that the waveform of a 70-ps impulse is well preserved. Theoretical computations using the method of moments and the FFT technique were performed and agreed well with time-domain measurements. The short "TEM" horn with continuously tapered resistive loading receives fast, time-varying, transient fields with minimal pulse-shape distortion due to nonlinear amplitude or phase characteristics of the transfer function. Although the antenna described in this paper was designed for a particular application, the theoretical design technique presented indicates that the approach can be used in other applications if extremely wide bandwidth and extremely low reflection coefficients are required.

REFERENCES

[1] M. Kanda, "The characteristics of a relatively short, broadband linear antenna with tapered resistive loading," *Int. Symp. Antenna Propagat. Digest,* pp. 230–233, Stanford Univ., CA (June 1977).

[2] M. Kanda, "A relatively short, cylindrical broadband antenna with tapered resistive loading for picosecond pulse measurement," *IEEE Trans. Antenna Propagat.*, AP-26, no. 3, pp. 439–447, May 1978.

[3] R. F. Harrington, *Field Computation by Moment Methods.* New York: The MacMillan Company, 1968.

[4] D. Wilton, "Digest of numerical and asymptotic techniques for electromagnetics and antennas," University of New Mexico, Mar. 1978.

[5] T. T. Wu, and R. W. P. King, "The cylindrical antenna with nonreflecting resistive loading," *IEEE Trans. Antennas Propagat.*, vol. AP-13, no. 3, pp. 369–373, May 1965.

[6] L. C. Shen, and T. T. Wu, "Cylindrical antenna with tapered resistive loading," *Radio Sci.*, vol. 2, no. 2, pp. 191–201, Feb. 1967.

[7] C. D. Taylor, "Cylindrical transmitting antenna: Tapered resistivity and multiple impedance loading," *IEEE Trans. Antenna Propagat.*, vol. AP-16, no. 2, pp. 176–179, Mar. 1968.

[8] C. E. Baum, "Resistively loaded radiating dipole based on a transmission line model for the antenna," *AFWL EMP 1-6, 6,* SSN-81, pp. 1–27, 1969.

[9] M. Kanda, "Transients in resistively loaded antennas and their comparison with conical antennas and TEM horns," *Int. Symp. Antenna Propagat., Digest*, 13–16, Univ. of Maryland, MD, May 1978.

[10] M. Kanda, "Transients in a resistively loaded antenna compared with those in a conical antenna and a TEM horn," *IEEE Trans. Antenna Propagat.*, vol. AP-28, no. 1, pp. 132–136, Jan. 1980.

[11] R. F. Harrington, *Time-Harmonic Electromagnetic Fields.* New York: McGraw-Hill Book Co., 1961.

[12] C. W. Harrison, Jr., and C. S. Williams, Jr., "Transients in wide-angle conical antennas," *IEEE Trans. Antenna Propagat.*, vol. AP-13, 236–246, Mar. 1965.

[13] R. W. P. King, *The Theory of Linear Antennas.* Cambridge, Massachusetts: Harvard University Press, 1956.

The Rhombic EMP Simulator

HAO-MING SHEN AND RONOLD W. P. KING, FELLOW, IEEE

Abstract—**A complete analysis has been carried out of the two-conductor rhombic antenna as an EMP simulator. The distribution of current along the conductors and the electric field in the working space bounded by rhombic wires have been determined at low, middle, and high frequencies. The analysis indicates that, at low frequencies, when the termination is the characteristic impedance, a traveling-wave current with very low standing-wave ratio propagates along the wires of the rhombic structure; but it is very sensitive to the load. As the frequency is increased, the standing-wave ratio also increases somewhat and it becomes less sensitive to the load. The electric field in the working space exhibits a reasonably constant amplitude with a standing-wave ratio of 1.5 or lower at all three frequencies.**

Key Words—**EMP simulator, rhombic, analysis.**

I. INTRODUCTION

An important EMP simulator of transmission-line type consists of a central parallel-plate section and tapered input and output regions, as shown in Fig. 1. These are constructed of sheet aluminum in a model simulator, such as the one at Harvard, or of wire mesh in the large structures used for actually testing aircraft. Simulators of this type are generally designed, in a quantitative sense, for the low-frequency end of the spectrum of frequencies actually of interest, with the hope they will be useful over the entire range. At the low frequencies, the plate separation and transverse dimensions of the simulator are electrically small so that radiation is negligible and the conventional transmission-line theory used in the design correctly applies. As the frequency is increased, radiation becomes significant and then dominant in limiting the amplitude of the current on the conductors. At all frequencies for which the distance between the parallel plates is not electrically small, transmission-line theory loses its validity. The termination which provides a traveling wave at low frequencies ceases to be effective at high frequencies since very little power actually reaches it—most of the power is radiated. As a consequence, standing waves occur and, because of the complicated geometry of the structure, an accurate analytical treatment that takes full account of radiation is excessively difficult. Approximate treatments involve higher modes that interact with the standing waves of the TEM mode to produce very deep minima (so-called notches)

Manuscript received September 30, 1981; revised January 15, 1982. This research was supported in part by the Joint Services Electronics Program under Contract N00014-75C-0648 with Harvard University.

The authors are with the Gordon McKay Laboratory, Harvard University, Cambridge, MA 02138. (617) 495-4468. H. M. Shen is a Visiting Scholar from the People's Republic of China.

0018-9375/82/0500-0255$00.75 © 1982 IEEE